NASA Technical Memorandum 83764

NASA-TM-83764 19840026159

An Experimental Investigation of the Effect of Boundary Layer Refraction on the Noise From a High-Speed Propeller

James H. Dittmar, Robert J. Burns, and Dennis J. Leciejewski
Lewis Research Center
Cleveland, Ohio

September 1984

NASA

AN EXPERIMENTAL INVESTIGATION OF THE EFFECT OF BOUNDARY LAYER REFRACTION ON THE NOISE FROM A HIGH-SPEED PROPELLER

James H. Dittmar, Robert J. Burns and Dennis J. Leciejewski
National Aeronautics and Space Administration
Lewis Research Center
Cleveland, Ohio 44135

SUMMARY

The noise generated by supersonic-tip-speed propellers is a possible cabin environment problem for future propeller driven airplanes. Models of such propellers were previously tested for acoustics in the Lewis 8- by 6-Foot Wind Tunnel using pressure transducers mounted in the tunnel ceiling. The boundary layer on the tunnel ceiling is believed to refract some of the propeller noise away from the measurement transducers. Measurements were made on a plate installed in the wind tunnel which had a thinner boundary layer than the ceiling boundary layer. The plate was installed in two locations for comparison with tunnel ceiling noise data and with fuselage data taken on the NASA Dryden Jetstar airplane. Analysis of the data indicates that the refraction increases with: increasing boundary layer thickness; increasing free stream Mach number; increasing frequency; and decreasing sound radiation angle (toward the inlet axis). At aft radiation angles greater than about 100° there was little or no refraction. Comparisons with the airplane data indicated that not only is the boundary layer thickness important but also the shape of the velocity profile. Comparisons with an existing two-dimensional theory, using an idealized shear layer to approximate the boundary layer, showed that the theory and data had the same trends. The theory appeared to overpredict the refraction effect and possibilities for theory improvement were indicated. Analysis of the data taken in the tunnel at two different distances from the propeller indicates a decay with distance in the wind tunnel at high Mach numbers but the decay at low Mach numbers is not as clear.

INTRODUCTION

The noise of high-tip-speed turboprops at cruise has been identified as a possible cabin noise problem for advanced turboprop airplanes. Scale models of this type of propeller have been previously tested for acoustics in the NASA Lewis 8- by 6-Foot Wind Tunnel using pressure transducers embedded in the wind tunnel wall (refs. 1 to 7). Some of these propeller models have also been flown on the NASA Dryden Jetstar airplane and noise measurements made by microphones installed flush in the airplane fuselage. Comparisons of the airplane and wind tunnel SR-3 propeller noise data (refs. 8 and 9) indicated that the noise measured in the wind tunnel fell off more rapidly from the peak toward the forward angles than did the airplane data. This difference in behavior was attributed to different amounts of boundary layer refraction that deflect the noise away from the measurement devices.

The boundary layer refraction phenomena was analyzed by Hanson (ref. 10) and the analysis indicated that the amount of refraction depends on the ratio of the sound wave length to an equivalent boundary layer thickness, the airflow Mach number, and the angle from the propeller (incidence angle of the

sound into the wall). It was suggested that the higher noise levels observed on the airplane for the SR-3 propeller at forward angles were because the boundary layer on the airplane was thinner than that in the tunnel which resulted in less refraction of the noise. Changes in the airplane configuration before testing the SR-6 propeller resulted in a different boundary layer that apparently resulted in boundary layer refraction characteristics like those in the tunnel since the SR-6 airplane-tunnel wall noise comparisons showed similar forward noise fall off (ref. 11).

The affect of boundary layer refraction on the measured noise of these model scale propellers may be larger than for full size propellers. In the larger size the wave length of the sound is longer and, with roughly the same fuselage boundary layer thickness, the noise passes through the boundary layer with less refraction than for a model propeller. The wall measured noise data for model propellers may thus result in less predicted noise when scaled up to full size than would be measured on a full size propeller.

To investigate the effect of the boundary layer refraction on the noise from scale model propellers, experiments were performed in the NASA Lewis 8- by 6-Foot Wind Tunnel with pressure transducers under two different boundary layers. One was the existing boundary layer on the wall of the wind tunnel and the other was a thinner boundary layer achieved on a plate in the tunnel freestream. This paper reports the different boundary layer characteristics tested and the different sound levels measured under those conditions and attempts to evaluate the parameters affecting boundary layer refraction.

APPARATUS AND PROCEDURE

Propeller

The eight bladed SR-3 propeller used in this test is nominally 0.622 m (24.5 in) in diameter. Table I shows some of the SR-3 propeller characteristics and more information on this propeller can be obtained from reference 12. A picture of this propeller installed in the NASA Lewis 8- by 6-Foot Wind Tunnel is shown in figure 1. Noise data from this propeller in the wind tunnel has been previously reported in references 1 to 3.

Transducer and Plate Locations

Noise measurements were made using pressure transducers installed in the tunnel ceiling and in a metal plate suspended from the ceiling. The transducers in the tunnel ceiling were installed, flush with the ceiling, through the tunnel bleed holes visible in figure 1. The locations of the tunnel ceiling transducers are shown in figure 2. These positions are the same as those previously tested in reference 3 except for position C which was inadvertently located on the opposite side of the ceiling centerline and slightly downstream for these experiments (see fig. 2).

A 2.54 cm (1 in) thick plate, 0.914 m (36 in) by 1.37 m (54 in), was installed in the wind tunnel at two different distances from the tunnel ceiling. The first location was just outside of the tunnel wall boundary layer which

was believed to be around 10.2 cm (4 in) thick at a tunnel Mach number of 0.8. The plate was installed on 12.7 cm (5 in) standoff supports so that a 12.7 cm (5 in) space existed under the plate and the surface of the plate was 15.24 cm (6 in) from the tunnel ceiling. Figure 3 shows the plate installed in the wind tunnel in this "close to ceiling" position.

The plate was also installed in a position to simulate the location of the fuselage during the airplane flight tests. Here the standoff supports were 38.48 cm (15.15 in) high so that the plate surface facing the propeller was 41.02 cm (16.15 in) from the tunnel ceiling. This results in the plate being 49.78 cm (19.6 in) or 0.8 diameter from the propeller tip. Figure 4 shows the plate installed in the wind tunnel in this "far from ceiling" position.

Pressure transducers were installed flush with the surface of the plate as shown in figure 5. Figure 5(a) shows a photograph of the plate with the transducer locations circled in white. A sketch of the plate with the geometric positions of the transducers and their identifying numbers is shown in figure 5(b). The positions marked with triangles on figure 5(b) were intended for comparison with data taken on the tunnel ceiling while those marked with squares were for comparison with the airplane data reported previously in references 8 and 9.

The transducers on figure 5(b) marked with triangles were to be operational when the plate was in the "close-to-ceiling" position. The close-to-ceiling positions, 4, 7, 10, and 13 were located using ray acoustics to be on the same ray as the tunnel ceiling positions A to D from reference 3. These positions were calculated using a ray which had its origin in the plane of rotation on a tangent to the propeller tip circle as it advances toward the observer position. These transducer positions were premachined into the plate before installation in the wind tunnel. Since transducer position C was placed on the opposite side of the tunnel centerline from that used in the calculation (mentioned earlier in this section) transducer position 10 is not located on the same ray as would intercept the actually tested position C.

The transducers numbered 2, 8, 11, and 15, also to be used when the plate was in the "close to ceiling" position, were chosen to be directly under the ceiling locations A to D. These positions were located and machined during the plate installation, so that transducer 11 does not suffer the same problem mentioned above for transducer 10 and transducer 11 was directly under ceiling transducer C.

Transducer positions 1, 3, 5, 6, 9, 12, and 14, shown with squares on figure 5(b) are used with the plate in the "far from ceiling" location. These positions are all located on the centerline of the plate which is directly above the propeller axis. These positions are for use in comparisons with the airplane data of reference 8. Positions 1, 3, 5, 6, 9, 12, and 14 correspond in order to the positions 2, 3, 4, 5, 6, 7, and 8 on the airplane fuselage listed in reference 8.

Boundary Layer Rakes

Boundary layer rakes were used to measure the boundary layer profiles on the tunnel wall and on the plate. The rake for the tunnel wall boundary layer

consisted of 14 tubes placed at the following distances from the tunnel ceiling: 0.163 cm (0.064 in), 0.488 cm (0.192 in), 0.978 cm (0.385 in), 1.63 cm (0.641 in), 2.44 cm (0.962 in), 3.419 cm (1.346 in), 4.559 cm (1.795 in), 5.862 cm (2.308 in), 7.328 cm (2.885 in), 8.956 cm (3.526 in), 10.747 cm (4.321 in), 12.7 cm (5.000 in), 14.653 cm (5.769 in), 16.606 cm (6.538 in). This rake was installed at position A and at position D (see fig. 2) to determine the wall boundary layer velocity profile.

A six tube rake was used to determine the plate boundary layer profile. This rake had tubes located at the following distances from the plate surface: 0.170 cm (0.067 in), 0.508 cm (0.200 in.), 1.02 cm (0.400 in), 1.69 cm (0.667 in), 2.54 cm (1.000 in), 3.39 cm (1.333 in).

The plate boundary layer rake locations are shown in figure 5(b). They correspond, axially, to positions 2 and 15 but were located 7.62 cm (3 in) on the opposite side of the plate centerline. The rake was installed in both fore and aft positions when the plate was in the "far from ceiling" location and was installed in only the aft position when the plate was in the "close to ceiling" location. A photograph showing the rake in the forward position on the plate is shown in figure 6. Acoustic data were not taken when the boundary layer rake was in place.

Operating Conditions

The wind tunnel was operated for both acoustic and boundary layer measurements, at 0.5, 0.6, 0.65, 0.7, 0.75, 0.8, and 0.85 Mach number. In addition the tunnel was operated at 0.55 and 0.9 Mach number for the boundary layer measurements on the tunnel wall. The propeller was operated at an advance ratio of 3.06 and a 3/4 radius blade setting angle of 61.3° for all of the acoustic tests at all tunnel Mach numbers and for the plate boundary layer tests. The propeller blades were replaced by a "dummy" spinner on the drive rig during the tunnel wall boundary layer measurements.

RESULTS AND DISCUSSION

Boundary Layer Measurements

Ceiling boundary layer. - The boundary layer thicknesses measured on the tunnel ceiling are found in table II(a). The thicknesses in table II are the distances from the wall where the velocity has reached 0.99 of the free stream velocity. The boundary layer thickness on the tunnel ceiling at the 0.8 axial Mach number was about 12.7 cm (5 in) at both forward and aft positions. The boundary layer profiles were, however, significantly different at the two measuring locations. An example of this can be seen in figure 7(a). At 0.8 axial Mach number, the aft position showed higher velocities near the ceiling and, contrary to expectation, showed a slightly thinner boundary layer than the forward position. The forward and aft boundary layer profiles differed at all tunnel Mach numbers but the aft boundary layer thickness was not always thinner (see table II(a)). The boundary layer profile indicated for the aft position is of the type expected for the porous test section of this tunnel. The holes in the wind tunnel connect to a balance chamber outside the tunnel. A fraction of the tunnel air is pulled out through these holes and the result

is higher velocities in the boundary layer near the wall than if the wall were solid. The forward boundary layer profile is more like that of a solid plate. Upon reexamination of the tunnel configuration, it was observed that the holes upstream of the forward rake position were partially blocked by a portion of the propeller drive rig support. This blockage can be seen in figure 6. In this photo the plugs which contain the ceiling pressure transducers are still installed. The photo is taken looking downstream in the tunnel and the tunnel bleed holes upstream of transducer A, forward rake location, can be seen to be partially blocked.

Transducer positions B and C can also be seen in figure 6. Position C has a number of open holes in front of it and probably has a boundary layer similar to that at the aft position, position D. The area in front of position B, however, is fairly solid and that position may have a boundary layer profile similar to that at the forward rake position.

Plate boundary layer. - The boundary layer thicknesses measured on the plate are tabulated in tables II(b) and (c). The boundary layer on the plate was also somewhat thicker than the rake was designed to measure. The profiles for the three positions on the plates at $M = 0.8$ are shown in figures 7(b) to (d). As can be seen at the last station on the rake the velocity has not reached 0.99 of the free stream velocity. Therefore to obtain an approximate boundary layer thickness the curves were extrapolated using a flat plate boundary layer profile shape, (ref. 13)

$$\frac{v}{v_\infty} = \frac{3}{2}\left(\frac{y}{\delta}\right) - \frac{1}{2}\left(\frac{y}{\delta}\right)^3$$

where v is the velocity in the boundary layer, v_∞ is the free stream velocity, y is the distance from the plate and δ is the boundary layer thickness.

The boundary layer profiles shown in figures 7(b) to (d) are typical for a flat plate and the forward rake shows a slightly thinner boundary layer thickness than the aft rake, as expected (table II(b)). The data at the aft position for the plate close to the wall is slightly different from that for the plate far from the wall (table II(c)). This may be a result of experimental error, an error arising from the extrapolation method or an indication of a slightly thinner boundary layer when the plate is in proximity to the wall. In any case, the difference is small. These results show that the boundary layers on the plate are about one-third of the wall boundary layer thickness.

Airplane boundary layer. - For comparison the boundary layer profile on the airplane test at $M = 0.8$ (refs. 8, 9, and 11) is again shown here in figure 8(a). This figure shows the boundary layer having higher velocities near the fuselage than would be expected from a flat plate boundary layer. Subsequent tests indicated that the airplane windshield wipers and supports acted as vortex generators and energized the airplane boundary layer. Reference 11 indicated that this profile apparently caused less boundary layer refraction than a boundary layer of roughly the same thickness but with a usual profile. Figure 8(b) shows the airplane boundary layer from figure 8(a)

plotted along with the forward position tunnel ceiling and plate boundary layer profiles.

Acoustic Data

Signals from the pressure transducers located in the ceiling and on the plate were recorded on magnetic tape. Narrowband spectra (0 to 10 000 Hz) with a bandwidth of approximately 26 Hz were taken for each of the test points. At some conditions, because of the low level of the blade passage tone or its closeness in frequency to tones from the wind tunnel compressor, narrowband spectra from 0 to 1000 Hz with a bandwidth of approximately 2.6 Hz were also taken. The tone levels were read from these narrowband plots and a compilation of the first eight harmonics is given in table III for the ceiling transducers, in table IV for the plate transducers when the plate was close to the ceiling, and in table V when the plate was far from the ceiling. As a result of transducer failure, transducer 14 was recorded in place of transducer 15 for the "close to ceiling" tests.

It should be noted here that the sound pressure levels measured on the ceiling for the SR-3 propeller during these tests were approximately 6 dB greater than those measured previously on the ceiling at the same conditions and reported in references 1 to 3. Exhaustive checks of the present instrumentation and calibration were performed after the discrepancy was noted and before the equipment was removed from the tunnel. The present data on the SR-3 propeller is therefore believed to be correct and the previous data, taken in conjunction with aerodynamic testing and reported in references 1 to 4, is apparently incorrect and should have approximately 6 dB added to all of the reported levels. The noise data for propellers SR-1M, 2, 5, and 6 (reported in refs. 1 and 2, and 5 to 7) used the same procedure and equipment as the previous SR-3 data and are probably also low by 6 dB.

Boundary Layer Refraction

Ceiling - plate close to ceiling. - The comparisons between the blade passage tone measured on the wind tunnel ceiling and that measured on the plate installed in the "close to ceiling" position are shown in figure 9. As can be seen in this figure, the tone noise directivity rolls off more rapidly at forward angles on the ceiling than on the plate. The roll off is also larger at the higher Mach numbers (figs. 9(a) to (c)) and increases as the measurement angle moves toward the propeller inlet axis. At the aft angles, greater than 100°, there is little or no difference between the ceiling and plate data. These effects can all be related to the thicker boundary layer on the tunnel ceiling which refracts the sound to a greater extent than does the thinner boundary layer on the plate. These results are, in general, the same as those indicated by the airplane tunnel comparisons of references 8 and 9.

As seen in figure 9, differences in the two sets of plate data were observed even for the transducers at the same angle (90°). There is no obvious explanation for these differences which are therefore presumed to be indicative of the data nonrepeatability.

The effect of the boundary layer refraction on the tone at twice blade passage frequency is shown in figure 10. Because of its lower sound pressure level relative to the tunnel background noise the harmonic is not discernable at as many angular positions or as many Mach number conditions as the blade passage tone. Also there seems to be somewhat a larger scatter in some of the harmonic data than in the blade passage tone data. From what is available, the general trends for the harmonic are similar to those for the blade passage tone. It appears that the refraction effect on the harmonic is as strong or possibly stronger than that on the blade passage tone.

Airplane - tunnel plate "far-from-ceiling" comparisons. - Comparisons of the normalized blade passage tone directivities measured on the NASA Dryden Jetstar airplane with those measured on the plate at the "far-from-ceiling" position, are shown in figure 11. Both the plate and the airplane fuselage were located at 0.8 propeller diameters clearance from the propeller tip.

The directivities shown in figure 11 are similar for both the airplane and plate data with only some local differences, for example at $M = 0.7$ at 80° and 100°. As noted before, when the airplane data were compared with data taken on the wind tunnel ceiling, the ceiling data showed significantly more refraction than the airplane data (refs. 8 and 9). The data taken on the plate in the wind tunnel show almost the same amount of refraction as the airplane data. This result would not be expected based on the relative boundary layer thicknesses determined at 0.99 of the free stream velocity. The airplane boundary layer at $M = 0.8$ (fig. 8(b)) appears to be much thicker than the plate boundary layer, and the refraction effects should be larger on the airplane if boundary layer thickness were the sole determining factor. The airplane and the wind tunnel ceiling boundary layer thicknesses are more nearly similar; yet, the airplane data showed considerably less refraction than the tunnel ceiling data (refs. 8 and 9). In short, the airplane data acts as if it were under a thinner boundary layer.

The reason the airplane boundary layer gives the refraction indicated for a thinner boundary layer is most likely associated with the boundary layer profile (fig. 8(b)). The airplane boundary layer does not have a typical profile since a portion of the boundary layer has been energized by the vortex generator action of the windshield wipers and support stands. It is probable that the portion of the boundary layer causing most of the refraction is that portion where the velocity gradients are large, i.e., the region from the wall out to about 2.5 cm (1 in). In this region the airplane boundary layer profile is very similar to the plate profile. Thus the airplane boundary layer has an "effective" thickness similar to the plate thickness and the apparently similar refraction properties are explainable. The present results indicate the importance of the profile shape in determining the amount of refraction and opens the possibility of contouring the boundary layer profile to reduce the noise reaching an airplane fuselage.

Theory - data comparison. - The amount of refraction provided by a boundary layer has been analyzed by Hanson (ref. 10). This analysis replaces the normal boundary layer profile with an idealized shear layer displaced some effective distance from the fuselage. The trends from the theory are that refraction occurs at the forward angles with hardly any at the aft angles, and that more refraction occurs at the higher through flow Mach numbers. These trends of the theory are consistent with those observed in the data that have

been presented. The data indicates more refraction with thicker boundary layers which is shown also in the theory. The dependency on frequency can be seen in the theory with higher frequencies giving shorter wavelengths and resulting in more refraction. This was also hinted at by the harmonic noise data of figure 10.

The predicted refraction cannot be directly compared with the data since free field (no refraction) data are not available. However, the theory can be used to predict the refraction for the ceiling and plate boundary layers present in this experiment. Then the difference for these two conditions can be compared with the measured noise differences from figure 9. As suggested by Hanson the equivalent shear layer depth can be taken as approximately the boundary layer thickness divided by eight. (This is approximately the momentum thickness for a typical boundary layer profile).

The boundary layer thicknesses for positions A (75°) and B (90.5°) on the tunnel ceiling were taken from the ceiling rake in the forward position and those for the positions C (102°) and D (110°) from the rear rake position (table II(a)). The boundary layer thicknesses on the plate in the 75° and 90.5° positions were taken from the front rake position (far from ceiling, table II(b)), and for the 101° and 110° locations from the rear rake position (close to ceiling, table II(c)). (The use of either front or rear boundary layer thicknesses makes less than a 0.5 dB difference in the predictions).

Calculations were performed for those cases where the theory predicted refractions (M = 0.7, 0.8) and the differences were taken between the ceiling and plate cases. Comparisons of the predicted and measured differences are shown in table VI for M = 0.7 and 0.8. Data differences are shown between the ceiling and plate curves for the plate transducers directly below the ceiling transducers and those determined by ray acoustics. As can be seen the predicted differences and the data differences have similar trends but the theory slightly overpredicts, possibly because it is a two-dimensional analysis that uses an idealized shear layer to approximate the boundary layer. A three-dimensional treatment using the velocity profile may be necessary to match the data. In particular a method using the specific velocity profile would appear to be needed to explain the behavior of the airplane boundary layer mentioned in the previous section. A three-dimensional analysis has been subsequently reported by Hanson (ref. 16). However, the required numerical solutions for these particular cases are not available at present for comparison with the data.

Decay With Distance

An indication of the tone noise decay rate with distance can be obtained by comparing the data with the plate close to the ceiling and that with the plate far from the ceiling. When the plate is in the far-from-ceiling position it is 1.3 propeller diameters from the centerline of the propeller (0.8 D tip clearance) and in the close-to-ceiling position it is 1.7 diameters from the centerline (1.2 D tip clearance). If 20 log of the ratio of the distances from the centerline is used as an expected sound decay rate, the data from the plate close to the ceiling should be approximately 2.3 dB less than the data taken from the plate far from the ceiling (1.7 dB results if the 15 log rate of shock decay is used, refs. 14 and 15). If the ratio of the tip clearances

is used, the difference should be 3.5 dB (2.6 dB if 15 log rate decay is used). The actual decay should probably be within these bounds since the point of origin of the tone noise is likely to be near the outer circumference of the propeller in the arc close to the plate.

The blade passage tones measured with the two plate positions are compared in figure 12. A number of interesting observations can be made from this figure. At the higher Mach numbers, 0.85 and 0.8 (figs. 12(a) and (b)) a definite decay with distance is observed at all positions. The amount of the decay does not appear to be a constant however. Rather it appears to vary with position and with the choice of the close plate transducer (position directly below, or determined by ray acoustics, see apparatus and procedure). This variation is probably an indication of the repeatability or experimental error of this data. The amount of this variation is large enough however that the data does not provide an answer as to the correct decay rate (20 log or 15 log) or the proper distance to be used.

As the through flow Mach number is reduced the amount of distance decay appears to decline. A possible reason for this may lie with increased tunnel wall reflection problems. Reference 17 has indicated some possible reasons why viable acoustic measurements have been obtainable on the walls of this wind tunnel, namely the high through flow Mach number and the sharp directivity of the propeller noise source. In particular, with the existing tunnel geometry, the reflected waves at the peak noise position from the opposite tunnel wall are swept downstream and strike the measuring wall downstream of the measurement transducer array. The reflected waves that do strike the array have origins in a portion of the directivity pattern that has lower noise. The reflected waves are swept further downstream with higher through flow Mach numbers. As the Mach number is decreased the amount of downstream sweep of the reflected sound becomes less and reflections may become more important.

It would normally be expected that measuring closer to a source would result in more exact data. However, in this case, it is the data at the "far-from-ceiling" position, closer to the source, which seem to have anomalies. For example, the "far-from-ceiling" data at $M = 65$ (fig. 12(e)) has a different directivity than normal. In front the data at the "far-from-ceiling" position is higher than the "close-to-ceiling" data by more than the expected decay, while the rear (around 100°) has a significant dip in the "far-from-ceiling" data. The directivity at this "far-from-ceiling" position is also significantly different than that at 0.5 or 0.6 Mach number (figs. 12(f) and (g)). It appears, possibly because of a poor combination of geometry, Mach number and source directivity, that the $M = 0.65$, "far-from-ceiling" data shows the effect of reflections from the opposite tunnel wall. In particular near 100°, which is the peak in the "close-to-ceiling" data, the dip in the "far-from-ceiling" data may be a result of an out of phase reflection from the wind tunnel wall.

CONCLUDING REMARKS

Experiments were performed, using a supersonic helical tip speed propeller as a noise source, to evaluate the effect of boundary layer refraction on the noise incident on a wind tunnel wall. Acoustic and boundary layer profile data were taken on the ceiling of NASA 8 ft by 6 ft wind tunnel and on a flat

plate installed at two different distances from the ceiling. The plate position close to the ceiling was designed to be just outside of the tunnel wall boundary layer and the plate position far from the wall was at the same 0.8 D tip clearance that the fuselage was located from the propeller during previous flight tests.

In comparison between the ceiling data, with a thicker boundary layer, and the plate close to the ceiling, with the thinner boundary layer, the ceiling data exhibited more boundary layer refraction. In general, the amount of boundary layer refraction increased with: increasing boundary layer thickness, increasing free stream Mach numbers, increasing frequency, and decreasing sound radiation angle (toward the inlet axis). At aft radiation angles greater than about 100° there was little or no refraction.

Comparisons between the plate far from the wall and the airplane fuselage data showed similar directivities. The airplane boundary layer appears to be considerably thicker than that on the plate so some noise difference, based on different boundary thickness, was expected. The airplane boundary layer does not exhibit a typical velocity profile, however, since it appears to have been partially energized by the vortex generator action of the airplane windshield wipers and supports. The similar behavior of the sets of data indicates the importance of not just the boundary layer thickness in determining the refraction but the velocity profile as well.

Comparisons of a two-dimensional boundary layer noise refraction analysis using an idealized shear layer approximation to the boundary layer with this data showed the theory to have the same general trends as the ceiling-plate comparison. Direct comparisons between theory and experiment were not possible since there are no zero thickness boundary layer data. The predicted differences between the ceiling and plate data were compared with the measured noise differences and although all of the correct trends were observed the theory slightly overpredicted the amount of refraction. It was indicated that improvements in the theory, to include three dimensions and a variable boundary layer velocity profile, might be needed to match the data, particularly in cases like the abnormally shaped airplane boundary layer profile.

Comparisons between the data taken far from the ceiling and near to the ceiling showed noise decay with distance at the higher Mach numbers. The trend at the lower Mach numbers was not as good. There was some indication that reflections from the opposite wind tunnel wall might have affected the 0.65 Mach number noise data taken with the plate far from the ceiling.

It should be noted that sound pressure levels measured on the ceiling for the SR-3 propeller during these tests are approximately 6 dB greater than those measured previously. Exhaustive checks of the present instrumentation and calibration were performed and the present data are believed to be correct. It is thereby indicated that the previous data on this SR-3 propeller are approximately 6 dB low. Data were taken using the previous equipment and procedure on four other propellers, SR-1M, SR-2, SR-5, and SR-6. It is therefore probable that if the previously taken SR-3 propeller data were low by 6 dB, the data from these four propellers were also low by 6 dB.

REFERENCES

1. Dittmar, James H., Blaha, Bernard J., and Jeracki, Robert J.: Tone Noise of Three Supersonic Helical Tip Speed Propellers in a Wind Tunnel at 0.8 Mach Number. NASA TM-79046, 1978.

2. Dittmar, James, H., Jeracki, Robert J., and Blaha, Bernard J.: Tone Noise of Three Supersonic Helical Tip Speed Propellers in a Wind Tunnel. NASA TM-79167, 1979.

3. Dittmar, James H., and Jeracki, Robert J.: Additional Noise Data on the SR-3 Propeller. NASA TM-81736, 1981.

4. Dittmar, James H., and Jeracki, Robert J.: Noise of the SR-3 Propeller Model at 2° and 4° Angle of Attack. NASA TM-82738, 1981.

5. Dittmar, James H., Stefko, George L., and Jeracki, Robert J.: Noise of the 10-Bladed, 40° Swept SR-6 Propeller in a Wind Tunnel. NASA TM-82950, 1982.

6. Dittmar, James H., Stefko, George L., and Jeracki, Robert J.: Noise of the 10-Bladed 60° Swept Propeller in a Wind Tunnel. NASA TM-83054, 1983.

7. Dittmar, James H., Stefko, George, L., and Jeracki, Robert J.: Noise of the SR-6 Propeller Model at 2° and 4° Angle of Attack. NASA TM-83515, 1984.

8. Dittmar, James H., and Lasagna, Paul L.: A Preliminary Comparison Between the SR-3 Propeller Noise in Flight and in a Wind Tunnel. NASA TM-82805, 1092.

9. Mackall, K. G., Lasagna, P. L., Walsh, K., and Dittmar, J. H.: In-Flight Acoustic Results from an Advanced-Design Propeller at Mach Numbers to 0.8. AIAA Paper No. 82-1120, June 1982.

10. Hanson, D. B.: Shielding of Prop-Fan Noise by the Fuselage Boundary Layer. HSER-8165, Hamilton Standard, 1981.

11. Dittmar, James H., Lasagna, Paul L., and Mackall, Karen G.: A Preliminary Comparison Between the SR-6 Propeller Noise in Flight and in a Wind Tunnel. NASA TM-83341, 1983.

12. Jeracki, Robert J., Mikkelson, Daniel C., and Blaha, Bernard J: Wind Tunnel Performance of Four Energy Efficient Propellers Designed for Mach 0.8 Cruise. NASA TM-79124, 1979.

13. Rohsenow, Warren M., and Choi, Harry Y.: Heat, Mass, and Momentum Transfer. Prentice-Hall, 1961, p. 29.

14. Energy Consumption Characteristics of Transports Using the Prop-Fan Concept. (D6-75780, Boeing Commercial Airplane Co.; NASA Contract NAS2-9104.) NASA CR-137937, 1976.

15. Dittmar, James H.: An Evaluation of a Simplified Near Field Noise Model for Supersonic Helical Tip Speed Propellers. NASA TM-81727, 1981.

16. Hanson, D. B.; and Magliozzi, B.: Propagation of Propeller Tone Noise Through a Fuselage Boundary Layer. AIAA Paper 84-0248, Jan. 1984.

17. Dittmar, James H.: Why Credible Noise Measurements are Possible in the Acoustically Untreated NASA Lewis 8 Foot by 6 Foot Wind Tunnel. J. Acoust. Soc. Am., vol. 75, no. 6, June 1984, pp. 1913-1914.

TABLE I. - SR-3 PROPELLER CHARACTERISTICS

Design cruise tip speed, m/sec (ft/sec)	244(800)
Design cruise power loading, kW/m^2 (shp/ft^2)	301(37.5)
Number of blades	8
Tip sweep angle, °	34
Predicted design efficiency, percent	81
Nominal diameter, D, cm (in)	62.2(24.5)

TABLE II. - BOUNDARY LAYER THICKNESS

(a) Tunnel ceiling

Rake position	Tunnel Mach number	Thickness, based on 0.99 velocity ratio, cm/in
Forward	0.5	13.84/5.450
	.55	13.72/5.400
	.6	14.65/5.769
	.65	14.99/5.90
	.7	14.22/5.60
	.75	13.84/5.45
	.8	12.95/5.10
	.85	13.21/5.20
	.9	12.95/5.10
Aft	0.5	14.65/5.769
	.55	12.95/5.10
	.6	15.49/6.10
	.65	15.88/6.25
	.7	15.24/6.00
	.75	12.7 /5.0
	.8	11.94/4.70
	.85	12.7 /5.0
	.9	12.95/5.10

(b) Plate far from ceiling

Forward	0.5	3.94/1.55
	.6	3.94/1.55
	.65	3.94/1.55
	.7	3.94/1.55
	.75	4.06/1.60
	.8	3.94/1.55
	.85	3.94/1.55
Aft	0.5	4.19/1.65
	.6	4.19/1.65
	.65	4.32/1.70
	.7	4.32/1.70
	.75	4.32/1.70
	.8	4.32/1.70
	.85	4.32/1.70

(c) Plate close to ceiling

Aft	0.5	4.06/1.60
	.6	4.06/1.60
	.65	4.06/1.60
	.7	4.06/1.60
	.75	4.19/1.65
	.8	4.19/1.65
	.85	4.06/1.60

TABLE III. - CEILING TRANSDUCERS

(a) M = 0.85; J = 3.06

Harmonic	Transducer			
	A	B	C	D
1	[a]122.0	142.5	144.0	152.5
2	(b)	131.0	142.0	137.5
3		(b)	134.5	141.5
4			(b)	132.5
5				132.0
6				128.0
7				123.0
8				122.0

(b) M = 0.80; J = 3.06

1	138.0	144.5	149.5	150.0
2	[a]126.5	137.0	144.0	144.5
3	(b)	132.0	134.0	135.0
4		(b)	138.5	139.0
5			128.5	129.5
6			131.0	131.5
7			120.5	121.0
8			122.0	122.5

(c) M = 0.75; J = 3.06

1	137.5	151.0	146.0	153.0
2	133.5	145.0	136.5	146.5
3	(b)	138.0	131.5	136.5
4		134.5	134.0	136.5
5		127.5	130.5	132.5
6		124.0	128.5	129.5
7		120.0	124.0	126.0
8		[b]	122.0	121.5

(d) M = 0.7; J = 3.06

1	140.0	149.0	146.5	144.0
2	135.5	142.5	140.0	148.0
3	130.0	138.5	138.0	134.0
4	(b)	133.0	131.0	129.0
5		131.0	130.5	129.5
6		126.5	128.5	125.0
7		122.0	125.0	120.0
8		118.5	124.0	118.0

(e) M = 0.65; J = 3.06

1	138.0	141.5	142.5	144.0
2	133.5	132.5	138.5	134.5
3	(b)	132.5	(b)	(b)
4		(b)		
5				
6				
7				
8				

TABLE III. - Concluded.

Harmonic	Transducer			
	A	B	C	D
1	132.5	140.0	135.0	133.0
2	(b)	(b)	(b)	(b)
3				
4				
5				
6				
7				
8				

(f) M = 0.6; J = 3.06

(g) M = 0.5; J = 3.06

1	122.0	123.0	(b)	121.5
2	(b)	(b)		(b)
3				
4				
5				
6				
7				
8				

[a]Only slightly above tunnel background.
[b]Not visible above tunnel background.

TABLE IV. - TRANSDUCERS ON PLATE CLOSE TO CEILING

(a) M = 0.85; J = 3.06

Harmonic	Transducer							
	2	4	7	8	10	11	13	14
1	[a]133.0	[a]132.5	149.0	146.0	140.5	143.5	154.5	154.5
2	(b)	(b)	137.0	136.0	146.0	143.0	138.5	139.5
3	↓	↓	(b)	(b)	132.5	138.5	142.5	144.0
4			↓	↓	129.0	130.0	136.0	131.0
5					125.5	128.0	133.0	135.5
6					121.5	123.5	131.5	130.0
7					121.0	118.0	123.0	125.0
8					119.0	118.0	123.0	125.5

(b) M = 0.8; J = 3.06

1	142.5	144.5	152.0	150.0	151.0	149.5	152.5	151.0
2	[a]134.0	[a]134.0	140.5	138.5	142.0	142.5	139.5	144.5
3	(b)	(b)	134.5	133.5	144.0	142.0	140.5	138.5
4	↓	↓	130.0	129.0	136.5	137.0	142.0	138.5
5			(b)	(b)	131.0	135.0	132.5	135.0
6			↓	↓	128.0	129.0	132.0	133.5
7					122.5	126.0	127.5	123.0
8						122.0	124.0	126.5

(c) M = 0.75; J = 3.06

1	146.0	146.0	152.0	154.5	154.5	152.0	152.5	150.0
2	140.5	138.0	149.0	142.0	148.0	143.5	150.5	148.0
3	[a]131.0	[a]132.0	139.5	139.5	137.5	133.5	136.0	138.5
4	(b)	(b)	134.5	136.5	138.5	135.0	138.0	139.0
5	↓	↓	130.0	129.0	132.5	130.0	134.5	137.0
6			127.5	126.5	132.0	131.5	130.0	132.5
7			123.5	122.0	127.0	126.5	126.0	129.5
8			[a]119.5	[a]118.0	125.0	124.5	123.5	126.0

(d) M = 0.7; J = 3.06

1	144.0	144.0	151.5	151.5	144.0	141.5	147.0	150.0
2	138.0	138.0	145.5	140.0	149.5	146.0	150.0	146.0
3	134.5	134.5	140.5	140.5	138.0	140.0	132.5	134.0
4	131.5	131.5	134.0	134.5	134.5	132.5	129.0	129.0
5	[a]126.0	[a]126.0	132.5	133.5	132.5	133.0	127.0	127.5
6	(b)	(b)	128.5	128.5	131.0	131.0	126.0	123.5
7	↓	↓	125.5	125.0	127.5	127.5	120.5	[a]120.5
8			123.0	122.0	126.5	126.5	120.5	119.0

(e) M = 0.65; J = 3.06

1	138.0	143.0	142.0	139.0	146.5	145.0	143.0	144.0
2	135.5	134.0	135.0	132.5	137.5	133.5	134.5	133.0
3	[a]131.0	[a]131.0	134.0	132.0	130.5	[a]130.0	[a]130.0	[a]130.0
4	(b)	(b)	126.5	126.5	(b)	(b)	(b)	(b)
5	↓	↓	124.5	123.0	↓	↓	↓	↓
6			(b)	[a]118.0				
7			↓	(b)				
8				(b)				

TABLE IV. - Concluded.

Harmonic	Transducer							
	2	4	7	8	10	11	13	14
(f) M = 0.6; J = 3.06								
1	130.0	127.0	140.0	137.5	139.0	138.5	137.0	135.0
2	(b)	(b)	(b)	(b)	(b)	(b)	(b)	(b)
3	↓	↓	↓	↓	↓	↓	↓	↓
4	↓	↓	↓	↓	↓	↓	↓	↓
5	↓	↓	↓	↓	↓	↓	↓	↓
6	↓	↓	↓	↓	↓	↓	↓	↓
7	↓	↓	↓	↓	↓	↓	↓	↓
8	↓	↓	↓	↓	↓	↓	↓	↓
(g) M = 0.5; J = 3.06								
1	(b)	120.0	124.5	123.5	124.5	127.0	124.5	125.0
2	↓	(b)	(b)	(b)	(b)	(b)	(b)	(b)
3	↓	↓	↓	↓	↓	↓	↓	↓
4	↓	↓	↓	↓	↓	↓	↓	↓
5	↓	↓	↓	↓	↓	↓	↓	↓
6	↓	↓	↓	↓	↓	↓	↓	↓
7	↓	↓	↓	↓	↓	↓	↓	↓
8	↓	↓	↓	↓	↓	↓	↓	↓

[a]Only slightly above tunnel background.
[b]Not visible above tunnel background.

TABLE V. – TRANSDUCERS ON PLATE FAR FROM CEILING

(a) M = 0.85; J = 3.06

Harmonic	Transducer						
	1	3	5	6	9	12	14
1	[a]133.5	(b)	136.0	150.5	143.5	155.5	157.0
2	(b)		(b)	141.5	147.0	136.0	152.5
3				133.0	135.5	141.5	145.0
4				(b)	129.5	139.5	146.0
5					[a]125.0	135.0	131.5
6					(b)	133.5	137.5
7						123.5	123.5
8						123.5	131.5

(b) M = 0.80; J = 3.06

1	141.0	145.5	147.5	154.5	152.0	157.0	156.0
2	(b)	[a]134.0	135.0	136.5	141.0	143.5	141.5
3		(b)	(b)	136.0	144.5	143.5	137.5
4				131.0	138.0	144.0	139.5
5				(b)	131.0	136.5	137.0
6					127.5	132.0	132.5
7					122.0	132.0	131.5
					(b)	125.0	127.5

(c) M = 0.75; J = 3.06

1	142.5	144.5	150.5	152.0	154.0	151.0	155.5
2	140.5	137.0	140.5	148.0	150.0	150.0	146.0
3	(b)	(b)	133.0	139.5	136.5	134.5	136.0
4			[a]129.0	138.0	138.0	141.0	138.5
5			(b)	132.5	135.0	139.5	136.0
6				128.5	133.5	134.0	129.0
7				124.0	129.5	131.0	127.0
8				120.0	126.0	125.5	123.5

(d) M = 0.70; J = 3.06

1	141.5	144.5	143.0	152.0	153.5	147.0	146.0
2	140.0	137.0	145.0	148.5	149.5	143.0	137.0
3	134.5	134.0	142.0	142.5	139.5	142.5	137.5
4	[a]129.5	129.0	135.0	136.5	132.0	134.0	129.5
5	(b)	(b)	131.5	136.0	133.0	133.0	129.5
6			127.0	132.0	129.5	131.5	125.0
7			122.5	128.5	127.5	127.5	[a]119.5
8			[a]118.5	125.0	127.0	125.5	[a]118.0

(e) M = 0.65; J = 3.06

1	140.0	144.0	148.5	147.0	141.0	142.5	145.5
2	133.0	137.5	133.5	139.5	141.0	140.0	134.5
3	(b)	[a]130.5	130.5	134.5	133.5	131.0	130.0
4		[a]126.0	122.0	127.0	126.5	(b)	(b)
5		(b)	123.5	123.0	(b)		
6			121.5	120.5			
7			118.5	120.0			
8			(b)	117.5			

TABLE V. - Concluded.

Harmonic	Transducer						
	1	3	5	6	9	12	14
(f) M = 0.6; J = 3.06							
1	123.5 (b)	130.0 (b)	138.0 (b)	140.0 (b)	140.0 (b)	137.5 (b)	134.0 (b)
2	↓	↓	↓	↓	↓	↓	↓
3	↓	↓	↓	↓	↓	↓	↓
4	↓	↓	↓	↓	↓	↓	↓
5	↓	↓	↓	↓	↓	↓	↓
6	↓	↓	↓	↓	↓	↓	↓
7	↓	↓	↓	↓	↓	↓	↓
8	↓	↓	↓	↓	↓	↓	↓
(g) M = 0.5; J = 3.06							
1	118.5[a] (b)	120.0 (b)	125.0 (b)	127.5 (b)	126.5 (b)	125.5 (b)	119.5 (b)
2	↓	↓	↓	↓	↓	↓	↓
3	↓	↓	↓	↓	↓	↓	↓
4	↓	↓	↓	↓	↓	↓	↓
5	↓	↓	↓	↓	↓	↓	↓
6	↓	↓	↓	↓	↓	↓	↓
7	↓	↓	↓	↓	↓	↓	↓
8	↓	↓	↓	↓	↓	↓	↓

[a]Only slightly above tunnel background.
[b]Not visible above tunnel background.

TABLE VI. - REFRACTION DIFFERENCES

Tunnel Mach number	Angle from axis, deg	Predicted refraction difference, dB	Measured refraction difference	
			Transducer positions directly below, dB	Transducer positions from ray acoustics, dB
0.8	75	11.5	5.5	6.5
	90	10.0	5.5	7.5
	101	2.0	0	1.5
0.7	75	9.0	5.0	4.0
	90	2.5	2.5	2.5

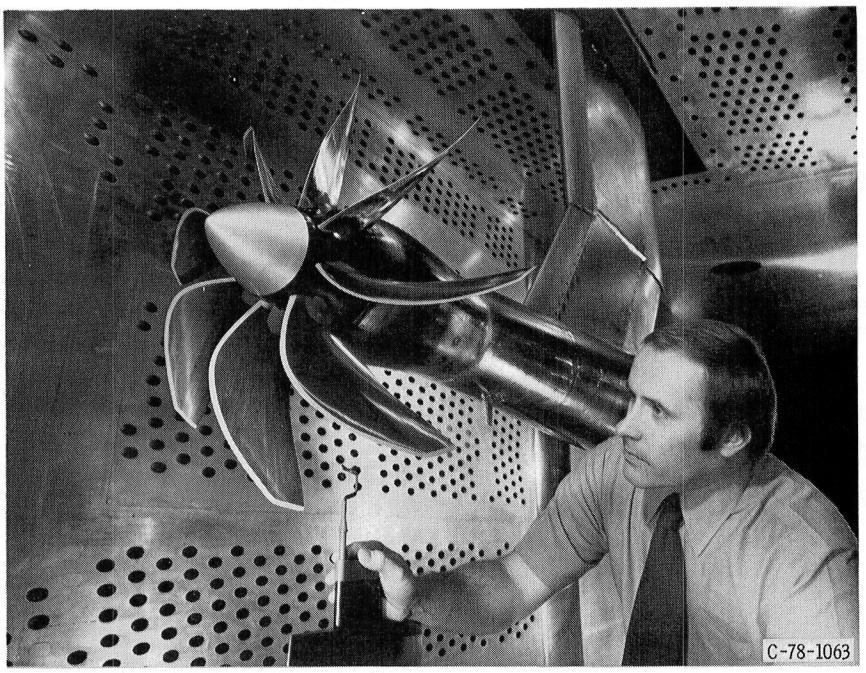

Figure 1. - SR-3 propeller in test section.

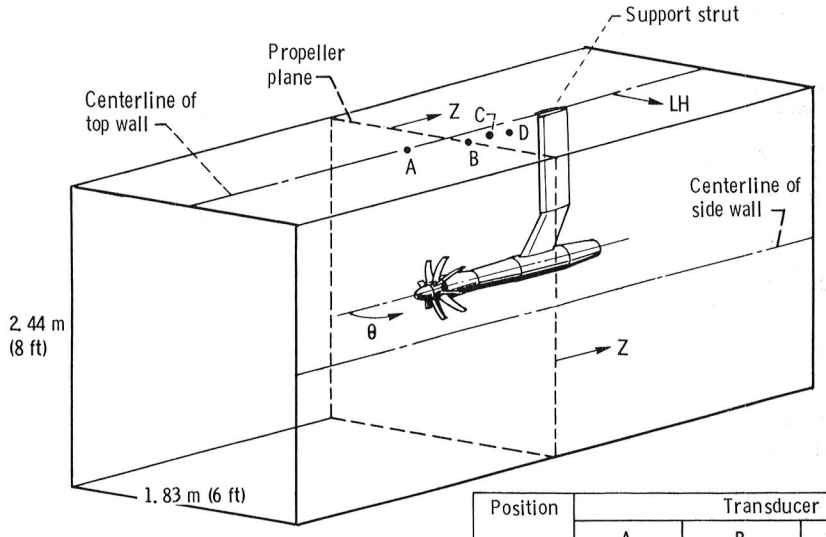

Position	Transducer			
	A	B	C	D
	Transducer position, cm (in.)			
Z LH	-33.0(13.0) 4.83(1.9)	0.953(0.375) 10.2(4.0)	25.7(10.1) -2.54(1.0)	45.2(17.8) 7.62(3.0)
Nominal angle, θ, deg	75	90.5	102	110

Figure 2. - Pressure transducer positions.

Figure 3. - Plate installed at close to ceiling position.

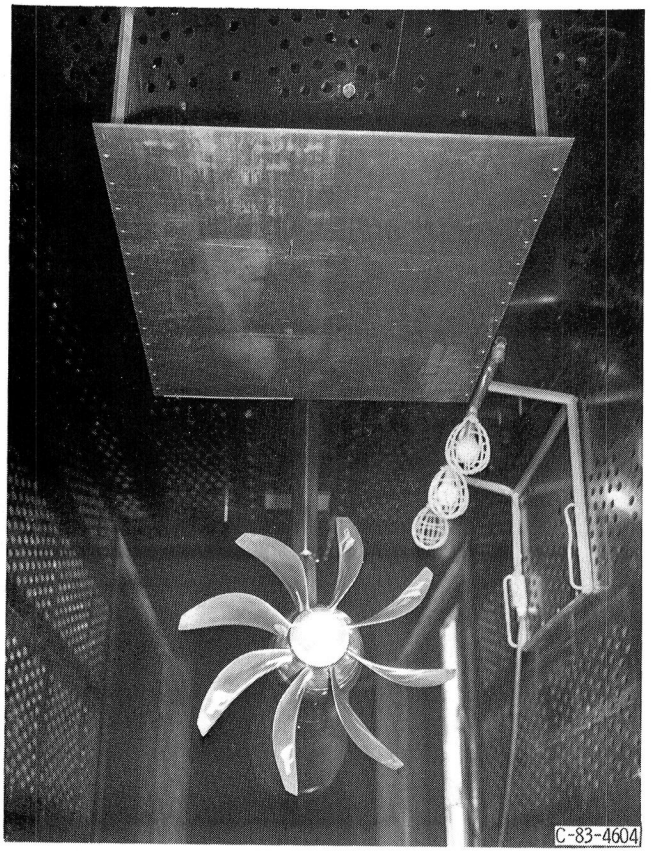

Figure 4. - Plate installed at far from ceiling position.

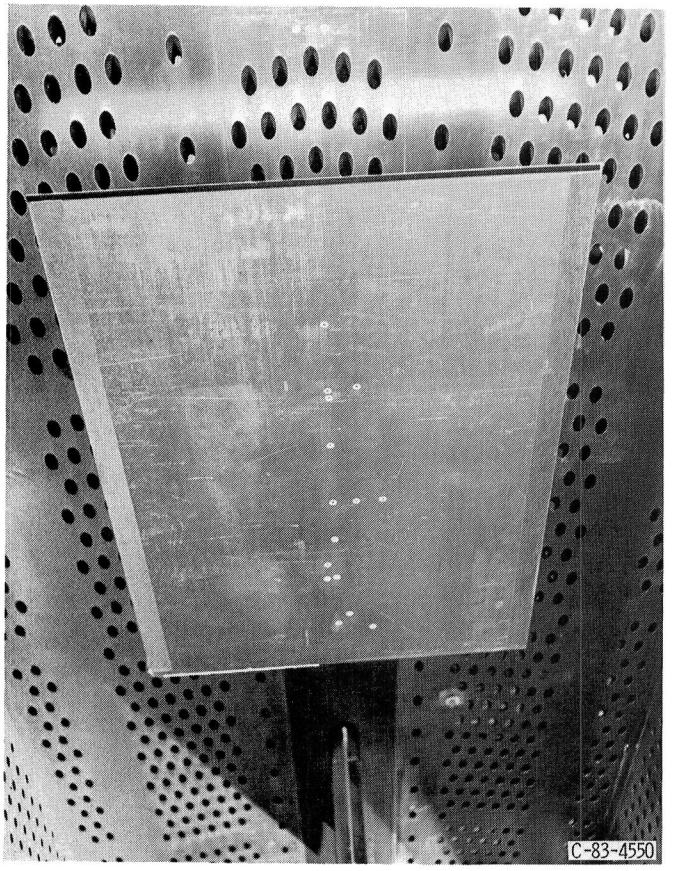

(a) Picture in tunnel.

Figure 5. - Plate transducer positions.

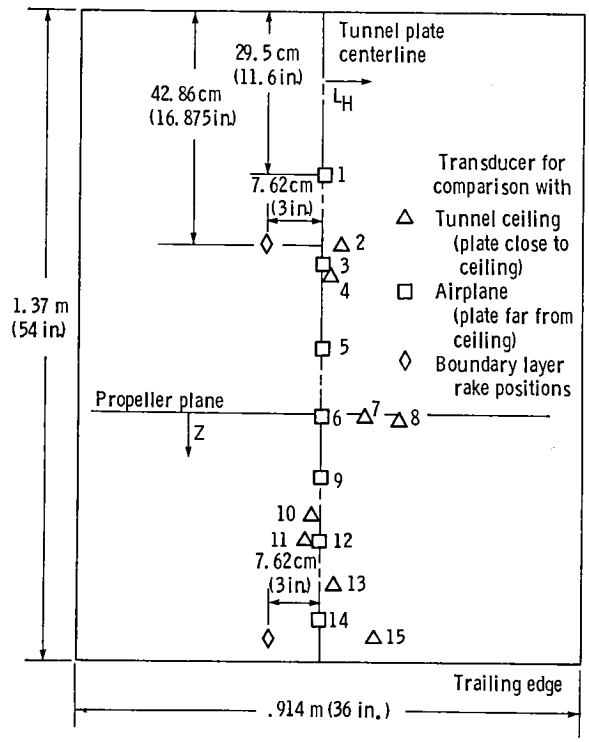

	Transducer														
	1	2	3	4	5	6	7	8	9	10	11	12	13	14	15
	Transducer position cm (in.)														
Z	-46.7 (-18.4)	-33.0 (-13.0)	-30.5 (-12.0)	-28.5 (-11.24)	-16.0 (-6.3)	.76 (.3)	.81 (.32)	.95 (.375)	12.4 (4.9)	20.7 (8.14)	25.7 (10.1)	25.1 (9.9)	39.1 (15.38)	42.4 (16.7)	45.2 (17.8)
L_H	0	4.83 (1.9)	0	.15 (.06)	0	0	4.78 (1.88)	10.2 (4.0)	0	-1.83 (-.72)	-2.54 (-1.0)	0	2.56 (1.01)	0	7.62 (3.0)
θ* Plate close	66.3	72.8	74.1	75.0	81.5	90.4	90.4	90.5	96.7	101.0	103.5	103.3	110.1	111.7	113.0
θ* Plate far	60.0	67.8	69.4	70.6	78.8	90.5	90.6	90.7	98.8	104.3	107.6	107.3	115.8	117.7	119.2

*Nominal angle from propeller axis using Z only.

(b) Sketch looking from below.

Figure 5. - Concluded.

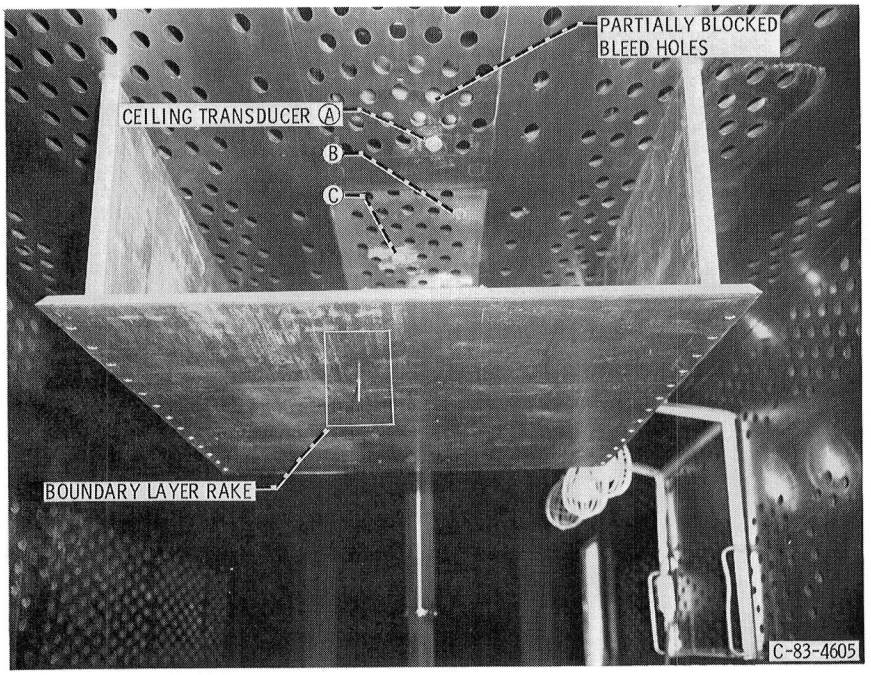

Figure 6. - Plate boundary layer rake.

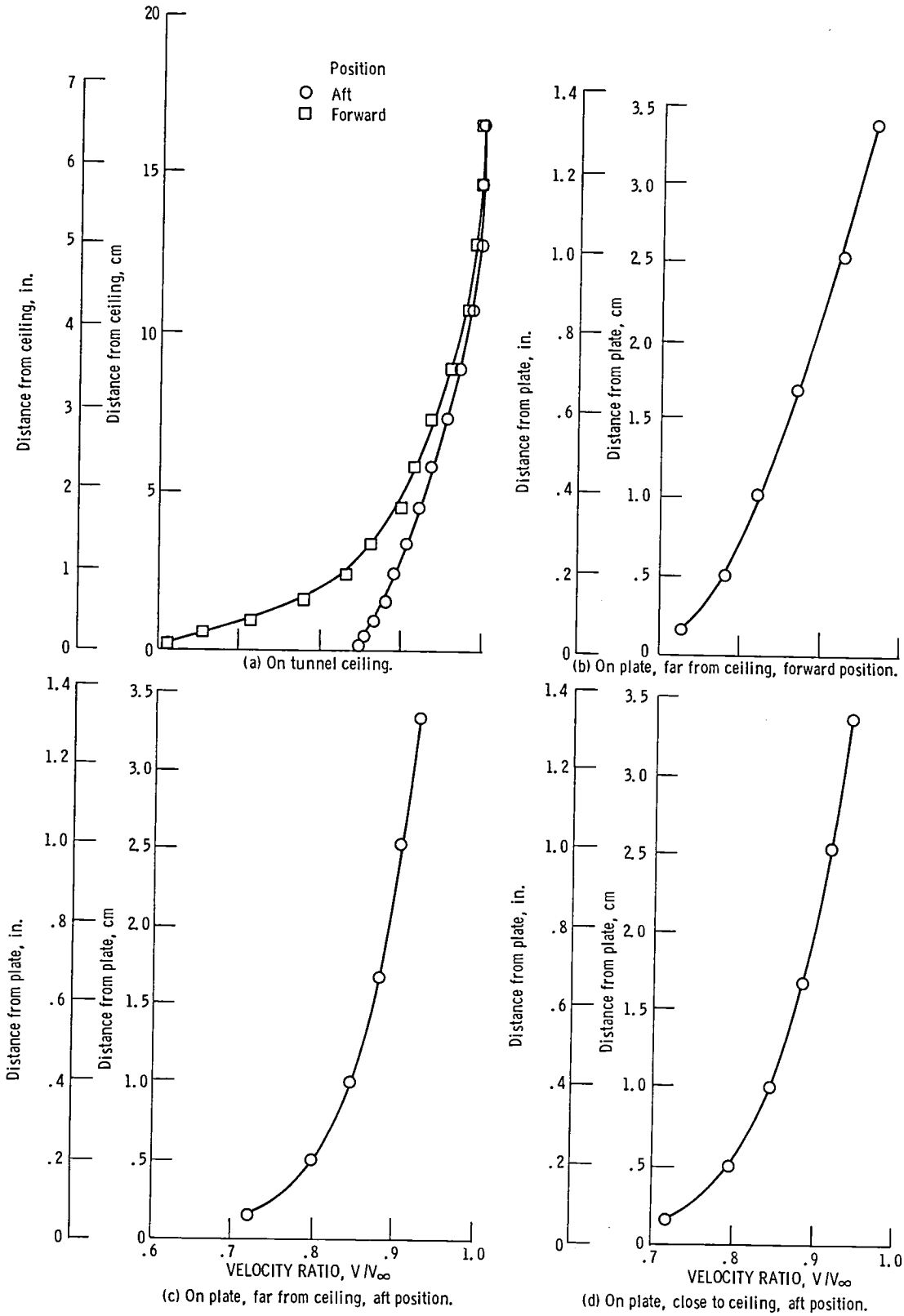

Figure 7. - Tunnel boundary layer profiles. Tunnel axial Mach number = 0.8.

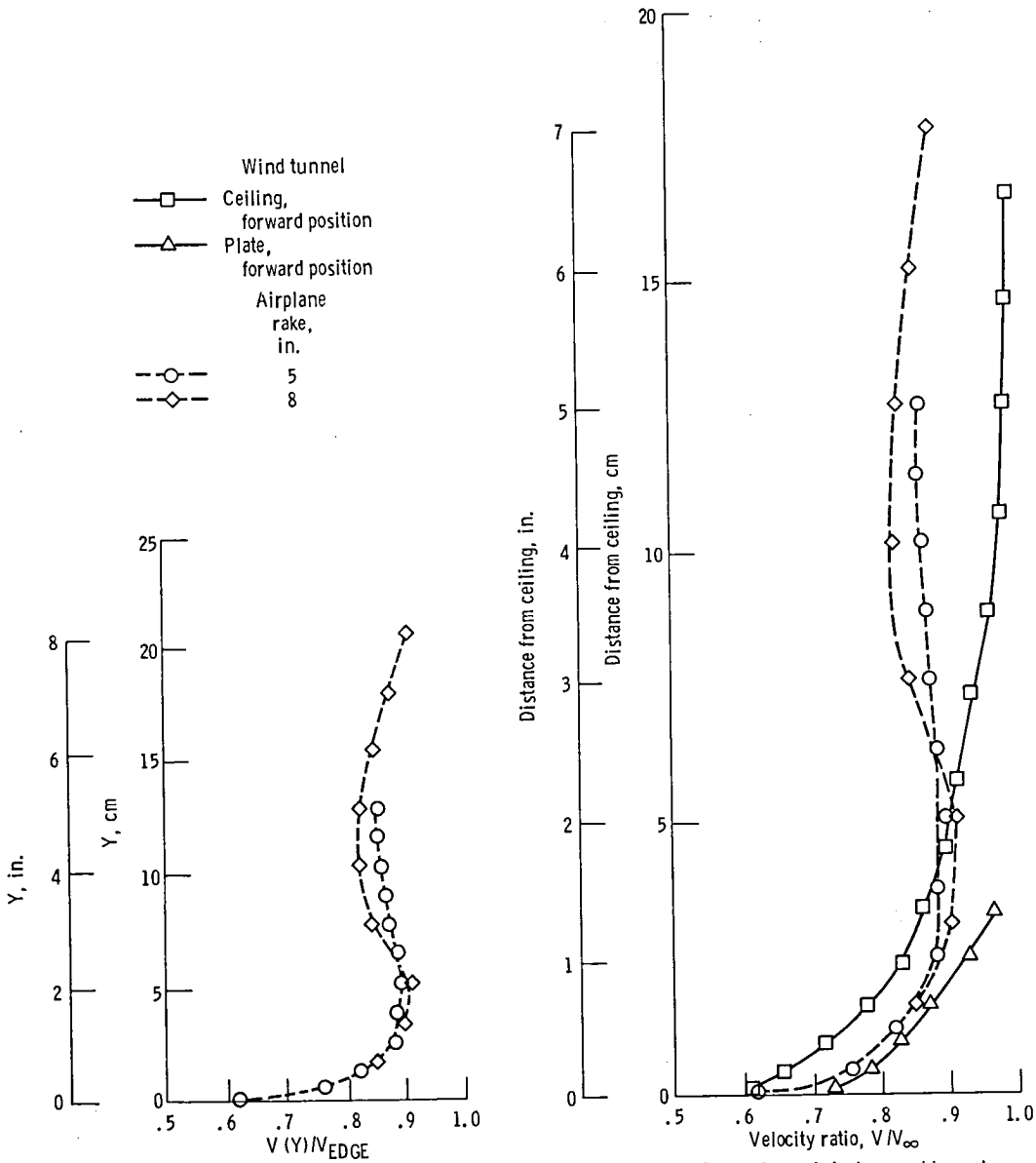

(a) Airplane boundary layer during SR-3 tests, with wipers; M = 0.8.

(b) Comparison of airplane and tunnel boundary layers at M = 0.8.

Figure 8. - Boundary layer profiles.

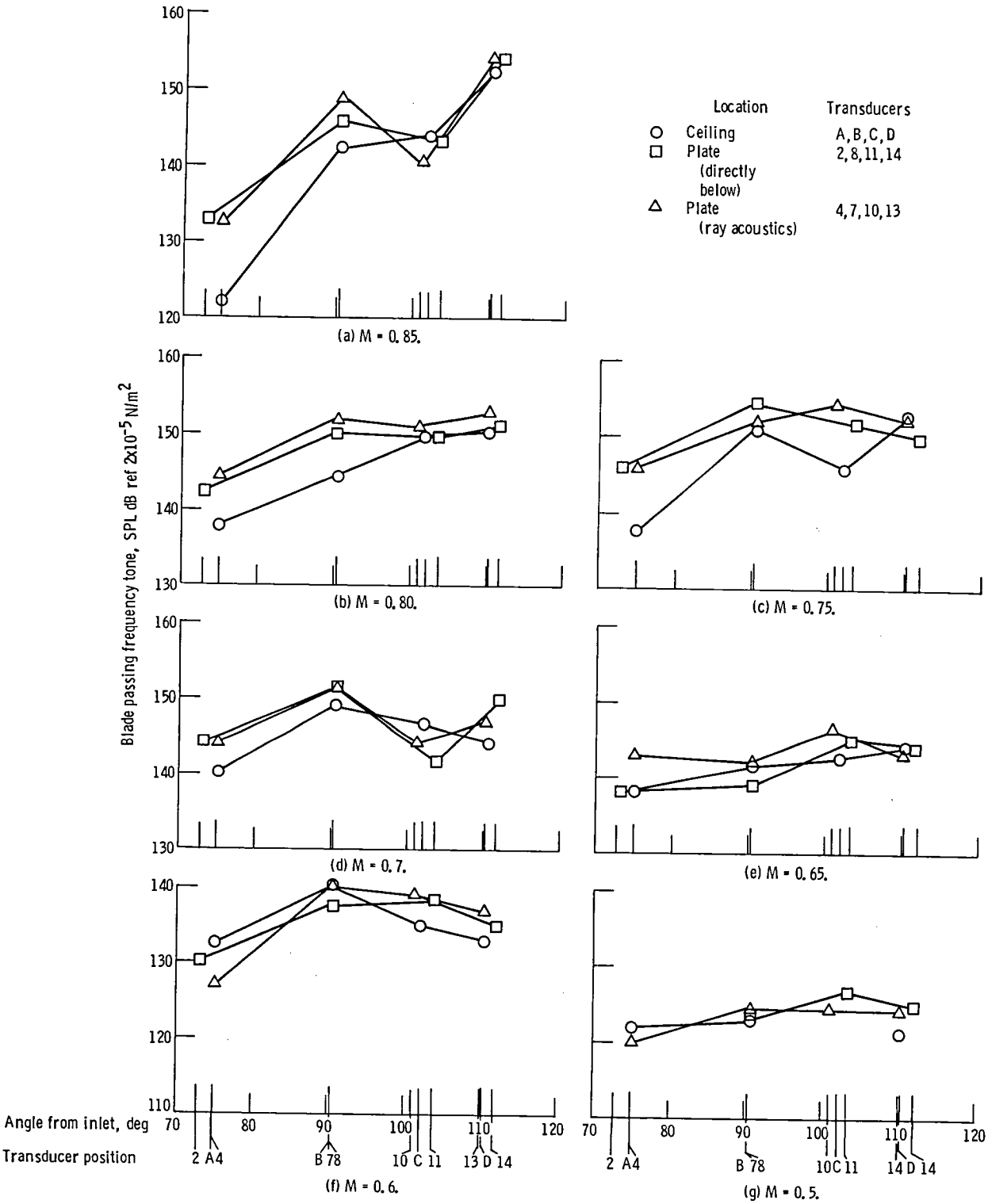

Figure 9. - Comparison of ceiling and plate tone at blade passage frequency (plate close to ceiling).

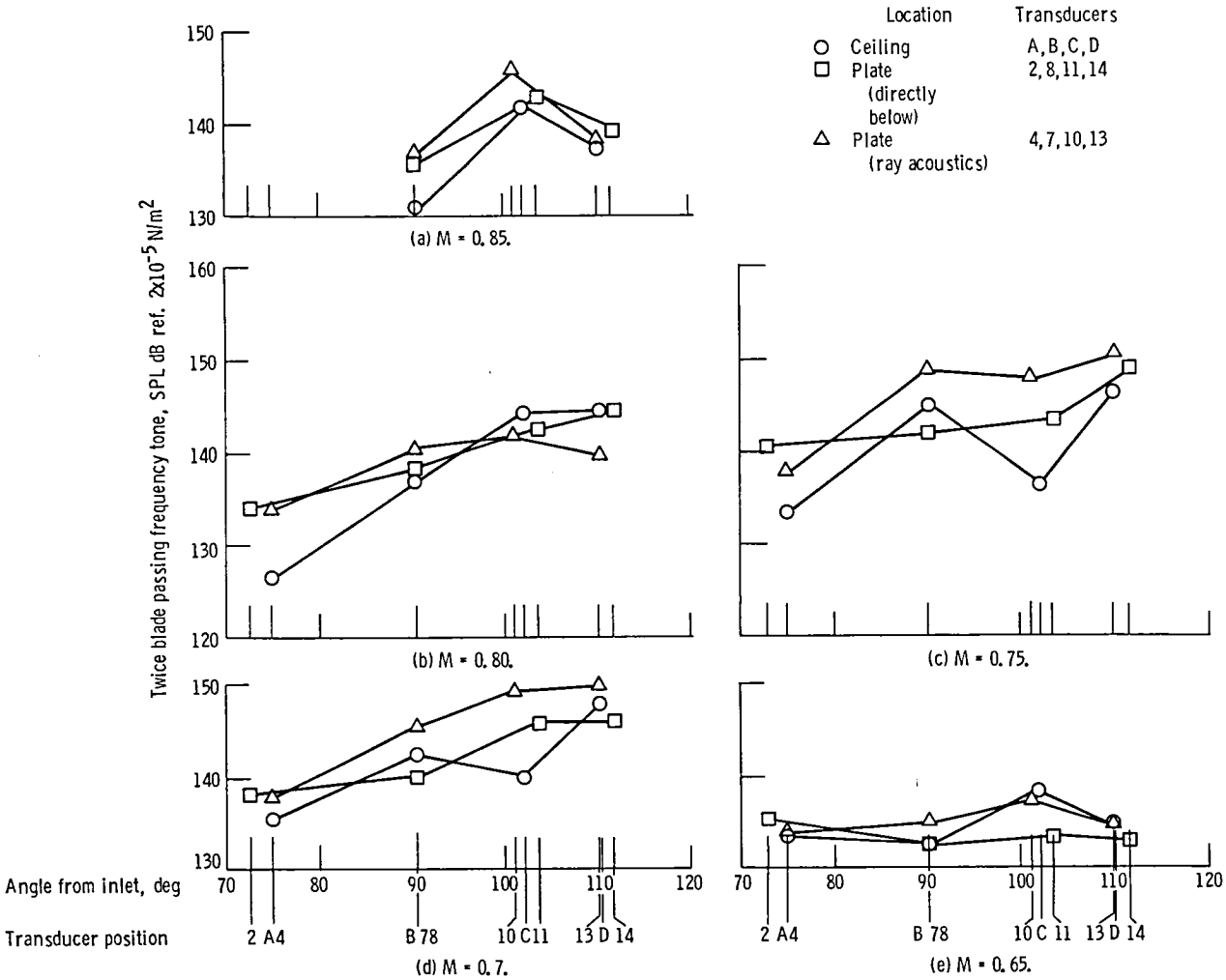

Figure 10. - Comparison of ceiling and plate tone at twice blade passage frequency (plate close to ceiling).

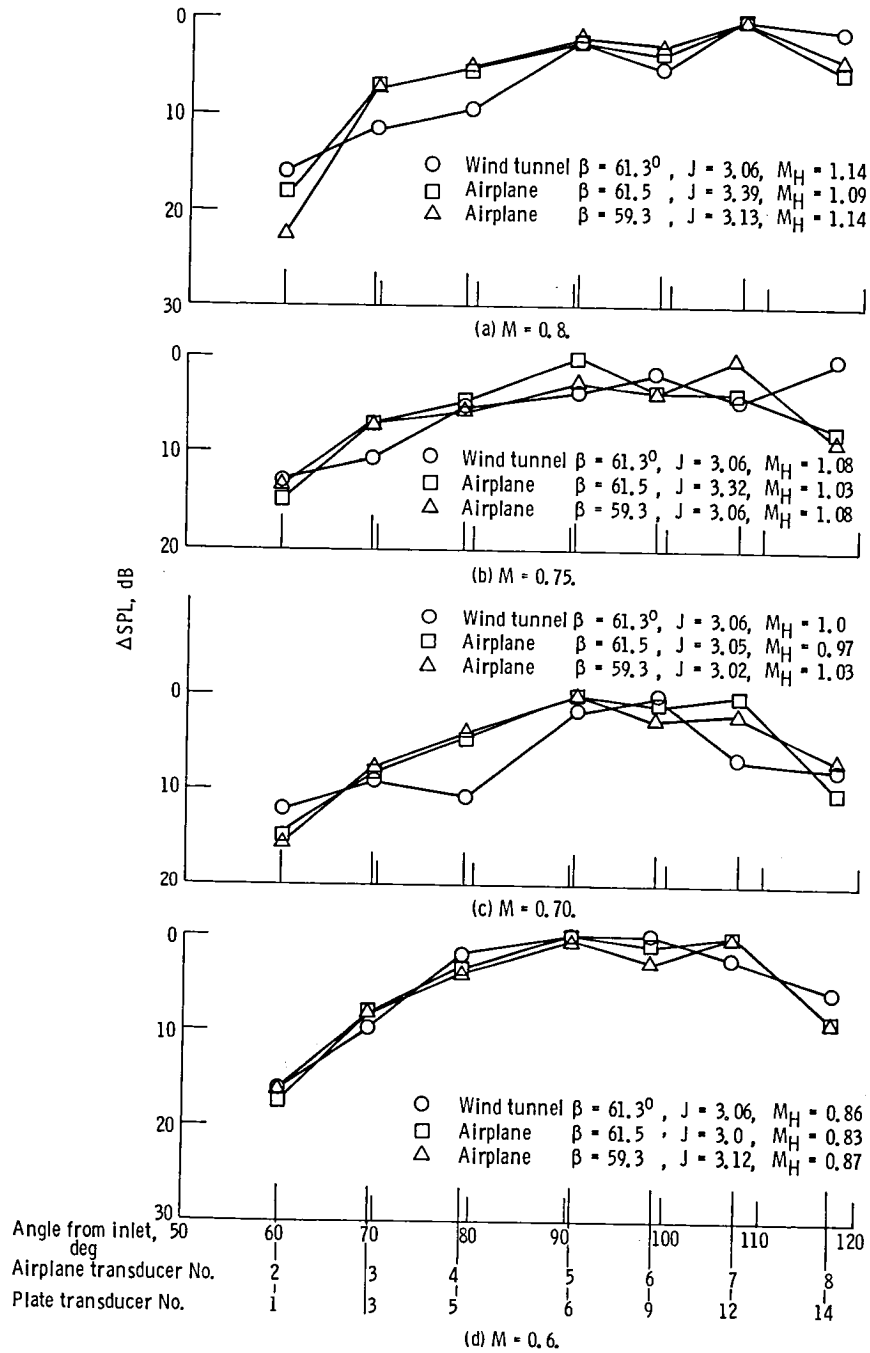

Figure 11. - Relative noise directivity comparison measured on the airplane fuselage and on the wind tunnel plate both at 0.8 D tip clearance.

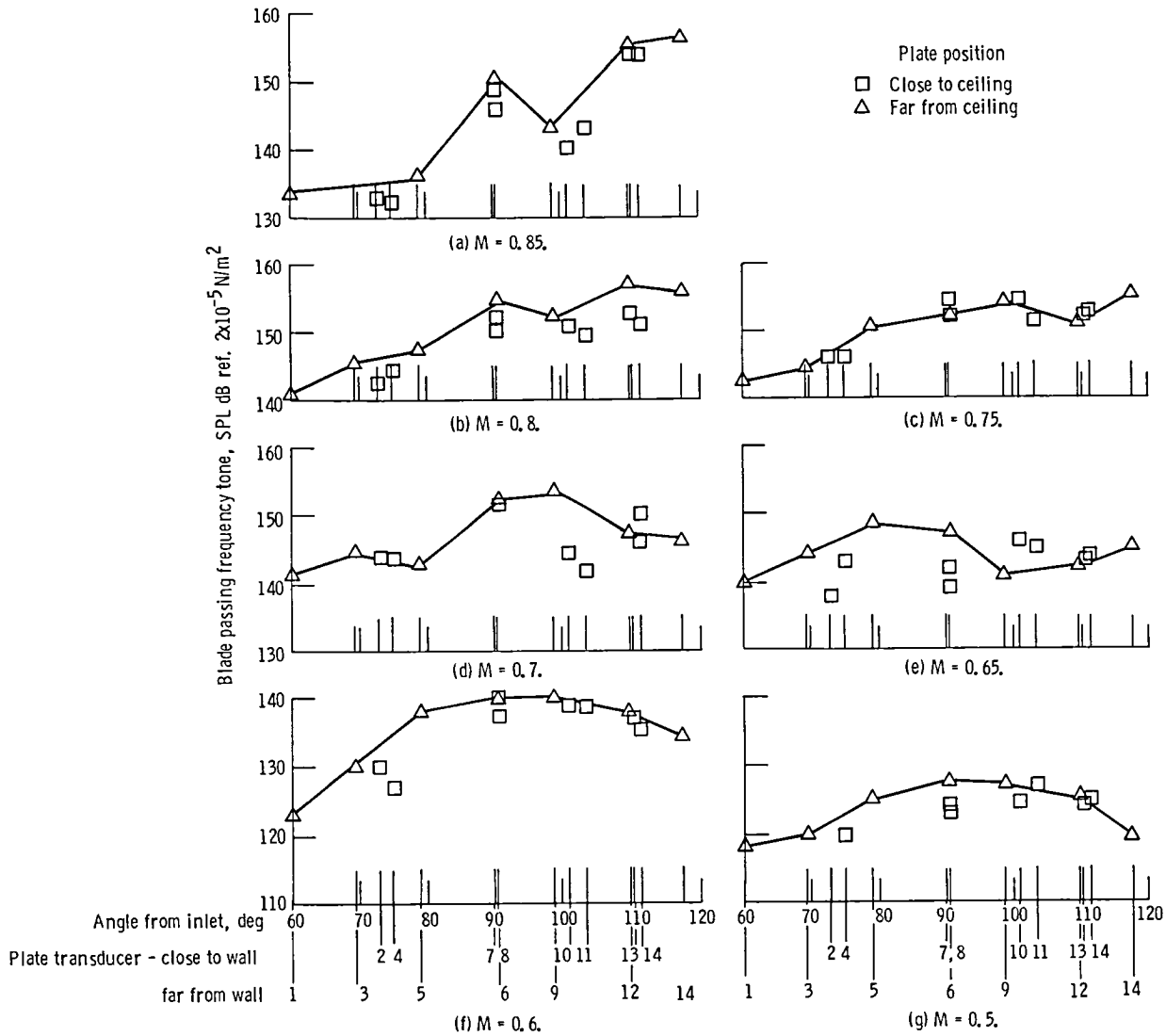

Figure 12. - Comparison of tone at blade passing frequency for plate close to ceiling with that of plate far from ceiling.

1. Report No.	2. Government Accession No.	3. Recipient's Catalog No.
NASA TM-83764		

4. Title and Subtitle
An Experimental Investigation of the Effect of Boundary Layer Refraction on the Noise From a High-Speed Propeller

5. Report Date
September 1984

6. Performing Organization Code
535-03-12

7. Author(s)
James H. Dittmar, Robert J. Burns, and Dennis J. Leciejewski

8. Performing Organization Report No.
E-2257

10. Work Unit No.

9. Performing Organization Name and Address
National Aeronautics and Space Administration
Lewis Research Center
Cleveland, Ohio 44135

11. Contract or Grant No.

13. Type of Report and Period Covered
Technical Memorandum

12. Sponsoring Agency Name and Address
National Aeronautics and Space Administration
Washington, D.C. 20546

14. Sponsoring Agency Code

15. Supplementary Notes

16. Abstract

The noise generated by supersonic-tip-speed propellers is a possible cabin environment problem for future propeller driven airplanes. Models of such propellers were previously tested for acoustics in the Lewis 8- by 6-Foot Wind Tunnel using pressure transducers mounted in the tunnel ceiling. The boundary layer on the tunnel ceiling is believed to refract some of the propeller noise away from the measurement transducers. Measurements were made on a plate installed in the wind tunnel which had a thinner boundary layer than the ceiling boundary layer. The plate was installed in two locations for comparison with tunnel ceiling noise data and with fuselage data taken on the NASA Dryden Jetstar airplane. Analysis of the data indicates that the refraction increases with: increasing boundary layer thickness; increasing free stream Mach number; increasing frequency; and decreasing sound radiation angle (toward the inlet axis). At aft radiation angles greater than about 100° there was little or no refraction. Comparisons with the airplane data indicated that not only is the boundary layer thickness important but also the shape of the velocity profile. Comparisons with an existing two-dimensional theory, using an idealized shear layer to approximate the boundary layer, showed that the theory and data had the same trends. The theory appeared to overpredict the refraction effect and possibilities for theory improvement were indicated. Analysis of the data taken in the tunnel at two different distances from the propeller indicates a decay with distance in the wind tunnel at high Mach numbers but the decay at low Mach numbers is not as clear.

17. Key Words (Suggested by Author(s))	18. Distribution Statement
Propeller noise Noise Boundary layer refraction Supersonic tip speed	Unclassified - unlimited STAR Category 71

19. Security Classif. (of this report)	20. Security Classif. (of this page)	21. No. of pages	22. Price*
Unclassified	Unclassified		

*For sale by the National Technical Information Service, Springfield, Virginia 22161